Polymer 55 (2014) 4837–4845

Contents lists available at ScienceDirect

Polymer

journal homepage: www.elsevier.com/locate/polymer

Synthesis of triarylamine-based alternating copolymers for polymeric solar cell

Jinhee Lee [a], Hyojung Cha [b], Hoyoul Kong [c], Myungeun Seo [d], Jaewon Heo [a], In Hwan Jung [a], Jisung Kim [a], Hong-Ku Shim [a], Chan Eon Park [b], **, Sang Youl Kim [a], *

[a] Department of Chemistry, KAIST, Daejeon 305-701, Republic of Korea
[b] Polymer Research Institute, Department of Chemical Engineering, Pohang University of Science and Technology (POSTECH), Pohang 790-784, Republic of Korea
[c] Korea Research Institute of Chemical Technology (KRICT), Division of Chemical R&BD at Ulsan, Ulsan 681-310, Republic of Korea
[d] Graduate School of Nanoscience and Technology KAIST, Daejeon 305-701, Republic of Korea

ARTICLE INFO

Article history:
Received 23 May 2014
Received in revised form
4 August 2014
Accepted 7 August 2014
Available online 15 August 2014

Keywords:
Triarylamine-based alternating copolymer
Benzothiadiazole derivative
Polymeric solar cell

ABSTRACT

Two donor-acceptor alternating copolymers based on electron-rich triarylamine, di(1-(6-(2-ethylhexyl))naphthyl)phenylamine (**DNPA**), and electron-deficient benzothiadiazole and benzoselenadiazole derivatives were designed and synthesized via Suzuki coupling reaction. The resulting triarylamine-based alternating copolymers **PDNPADTBT** and **PDNPADTBS** showed good solubility in common organic solvents and good thermal stability. The optical band gaps determined from the onset absorption were 1.93 and 1.81 eV, respectively. By introducing the naphthalene ring into the triarylamine, copolymers had relatively deep HOMO energy levels of −5.48 and −5.45 eV, which led to a high open circuit voltage (V_{oc}) and good air stability for photovoltaic application. Bulk heterojunction solar cells were fabricated with a structure of ITO/PEDOT-PSS/copolymers-$PC_{70}BM$/LiF/Al by blending the copolymer with $PC_{70}BM$. Both blend systems showed remarkably high V_{oc} near 0.9 V, and the highest performance of 2.2% was obtained from **PDNPADTBT**, with $V_{oc} = 0.88$ V, $J_{sc} = 7.4$ mA/cm^2, and a fill factor of 34.4% under AM 1.5 G.

1. Introduction

Efforts to find sustainable energy sources have led development of new renewable energy technologies which use wind power, geothermal heat, tidal power, and solar energy [1]. Among them, solar energy has been studied intensively for decades to transform sunlight into electrical energy and various types of solar cells were designed on the basis of materials [2–6]. Polymer-based organic solar cells (PSCs) have attracted scientific interest owing to its low cost, easy processability, portability, and ability to make large-area devices [7,8]. Particularly, fabrication of PSCs with a bulk heterojunction structure, typically a bicontinuous network of electron-donating polymer and electron-acceptor such as phenyl-C61-butyric acid methyl ester ($PC_{61}BM$), has enhanced charge separation and transportation and therefore significantly increased power conversion efficiency (PCE) close to a level required for commercialization [9]. Furthermore, concurrent increase in short circuit current (J_{sc}) and open circuit voltage (V_{oc}) have been realized by development of low band gap conjugated polymers which consist of electron-rich donors and electron-deficient acceptors in the polymer main chains in an alternating fashion, which resulted low HOMO energy levels and low band gaps via push–pull effect [10]. PCE values up to 8% have been reported by using low band gap alternating copolymers [11–15].

Triarylamine is a well-known electron-rich moiety that readily interacts with electron-deficient acceptor species via charge-transfer interaction and also undergoes oxidation to form stable radical cation species [16]. Many triarylamine derivatives have been widely investigated and applied in various electro-optical materials such as organic light-emitting diodes (OLEDs), organic field-effect transistors (OFETs), organic solar cells (OSCs), and dye-sensitized solar cells (DSCs) [17–20]. Especially, excellent electron-donating ability of the triarylamine moiety was intensively exploited for bulk heterojunction OSC and PSC applications [21–33]. Moreover, recent reports have suggested that triarylamine-based alternating copolymers could be promising candidates for donor material due to its amorphous film formability and highly reproducible performances [34–36]. However, there have been only few papers on

---

* Corresponding author. Tel.: +82 42 350 2834.
** Corresponding author. Tel.: +82 54 279 2269.
E-mail addresses: cep@postech.ac.kr (C.E. Park), kimsy@kaist.ac.kr, polysky@gmail.com (S.Y. Kim).

http://dx.doi.org/10.1016/j.polymer.2014.08.018
0032-3861/

incorporating triarylamine moieties with an electron-deficient acceptor along the conjugated backbone to achieve low band gap polymers [34–43]. Among them, copolymers composed of triphenylamine and 2,1,3-benzothiadiazole (BT) derivatives showed remarkable result, but they showed relatively high HOMO level and solubilizing groups on BT derivatives were required due to low solubility [34,36–38,40,41].

To this end, we designed new low band gap conjugated polymers consisting of a triarylamine moiety. The target polymer structure is shown in Fig. 1. Replacement of the phenyl rings of the triphenylamine with other aromatic rings such as naphthalene could be a quite efficient method to control the energy level of the copolymer, and Kwon group has reported incorporation of naphthyl groups lowers the HOMO energy level of the copolymers and increase V_{oc} of the solar cell devices [35,44,45]. From this point of view, we introduced two (2-ethylhexyloxy)-naphthyl groups to the triarylamine moiety to render solubility of the copolymer and further control the HOMO energy level and V_{oc}. Meanwhile, we chose BT unit as electron-deficient moiety to form alternating copolymer with the triarylamine moiety. It has been proved that BT is excellent electron-deficient unit and successfully incorporated in low band gap conjugated polymers for electroluminescent and photovoltaic applications [46,47]. In addition, to enhance association between the polymer chains, we designed to increase conjugated length of the electron-deficient moiety by introducing two thiophene rings at both sides of BT unit [48]. Its analog 2,1,3-benzoselenadiazole (BS) was also incorporated into the copolymer as electron-deficient unit. BS containing polymers are known to be more effectively moving the absorption of light toward the longer wavelength region than BT while its HOMO energy level remains similar value with BT [49–51]. Therefore, it is expected that BS based polymers are more efficient to harvest solar energy, but the photovoltaic performance of polymers-based on carbazole and 4,7-di-2,1,3-benzoselenadiazole (DTBS) units lagged behind result that of 4,7-di-2-thienyl-2,1,3-benzothiadiazole (DTBT) [52]. Thus, we developed new triarylamine-based alternating copolymers and compared the effect of BT and BS on the properties of copolymers.

In this study, a new triarylamine-containing di(boronic ester) monomer was synthesized and corresponding alternating copolymers with BT- or BS-containing dibromo monomers were successfully produced via Suzuki coupling. Properties of the polymers and photovoltaic characteristics of bulk heterojunction PSCs fabricated by blending the polymers with $PC_{70}BM$ as an acceptor were investigated.

2. Experimental

2.1. Materials

All chemicals were purchased from commercial sources (Aldrich, TCI, or Junsei) and used without further purification. The following compounds were synthesized according to the procedures in the literature: 5-iodo-2-naphthol (**2**), 4,7-bis(5-bromo-2-thienyl)-2,1,3-benzothiadiazole (**6**), and 4,7-bis(5-bromo-2-thienyl)-2,1,3-benzoselenadiazole (**7**) [49,53–55].

2.2. Material characterization

The Fourier-transform infrared (FTIR) spectra of the copolymers were obtained with a Burker EQUINOX-55 spectrophotometer using a KBr pellet. ^{1}H and ^{13}C NMR spectra of synthesized materials were recorded on a Bruker Fourier Transform AC 400 (400 MHz) spectrometer. Chemical shifts were expressed in part per million (ppm) with reference to the peak of residual DMSO (2.49 for ^{1}H and 39.52 ppm for ^{13}C) and $CHCl_3$ (7.24 ppm for ^{1}H and 77.16 ppm for ^{13}C), respectively. Mass spectra were obtained with a Bruker Daltonik microTOF-QII mass spectrometer using electrospray ionization (ESI) method, and elemental analysis was conducted using a Thermo Scientific FLASH 2000 series elemental analyzer. Molecular weights and molecular weight distributions of polymers were measured by the means of size exclusion chromatography (SEC). The SEC diagrams were obtained with Viscotek TDA302 equipped with a RI detector and three packing columns (PLgel 10 μm MIXED-B) using tetrahydrofuran (THF) as an eluant at 35 °C. The number- and weight-average molecular weights of the polymers were calculated relative to linear polystyrene standards. Thermogravimetric analysis (TGA) and differential scanning calorimetry (DSC) were conducted on a TA Instruments TGA Q500 and a DSC Q2000, respectively. The TGA and DSC measurements were performed under nitrogen atmosphere at a heating rate of 10 °C/min. UV/vis spectra were measured on a JASCO V-530 and an Optizen Pop spectrometer. Films for the UV-vis measurements were prepared by spin coating of the polymer solution in chloroform (1 wt%). Cyclic voltammetry (CV) was performed on an AUTOLAB/PG-STAT12 model with a three-electrode cell in a solution of tetrabutylammonium tetrafluoroborate (Bu_4NBF_4) (0.1 M) in acetonitrile at a scan rate of 50 mV s^{-1}. A film of each polymer was coated onto a Pt wire electrode by dipping the electrode into a solution of the polymer. The Ag/Ag^{+} reference electrode was calibrated using a ferrocene/ferrocenium redox couple as an internal standard, whose oxidation potential is set at −4.8 eV with respect to zero vacuum level.

2.3. Device fabrication and characterization of PSCs

PSCs were fabricated with the structure glass/indium tin oxide (ITO)/poly(3,4-ethylenedioxythiophene):poly(styrenesulfonate) (PEDOT:PSS)/polymer:$PC_{70}BM$/LiF/Al in the N_2 globe box. The glass substrate with pre-patterned ITO (Freemteck, resistance: 10 Ω/square) active layer with a thickness of 0.09 mm^2 was ultrasonicated in detergent, D.I. water, CMOS-grade acetone, and isopropanol, and the surface of the glass substrate was modified with UV-ozone treatment for 20 min. PEDOT:PSS (Bay P VP AI4083, Bayer

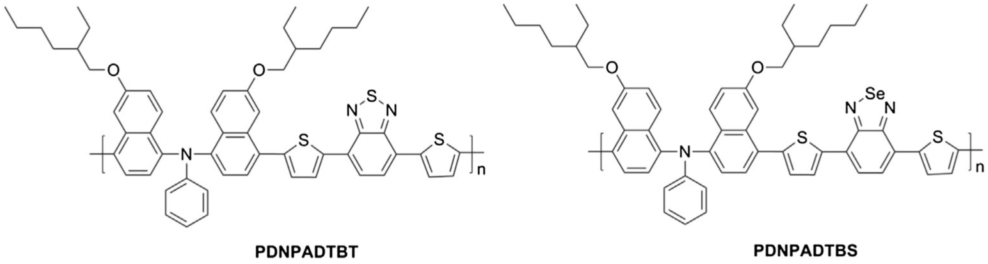

Fig. 1. Low band gap conjugated polymers consisting of triarylamine moiety.

AG) was spin-coated for hole injection at 4000 rpm for 60 s to a thickness of 30–40 nm on the cleaned ITO-patterned glass substrate after filtration through a 0.45 μm filter, followed by baking in an oven at 120 °C for more than an hour. The blended solutions were spin-coated onto the above substrate at 1000 rpm for 60 s to a thickness of 100 nm. The LiF and Al cathodes were thermally deposited to thicknesses of 1 and 100 nm, respectively, onto the surface of the active layer. The current density-voltage (*J*–*V*) characteristics of the device were measured using a Keithley 4200 source measurement unit, in the dark and under AM 1.5 G solar illumination (Oriel 1 kW solar simulator) with respect to a reference cell PVM 132 calibrated at the National Renewable Energy Laboratory, at an intensity of 100 mW/cm^2. External quantum efficiency (EQE) was measured using a photomodulation spectroscopic setup (model Merlin, Oriel), a calibrated Si UV detector, and an SR570 low noise current amplifier. The atomic force microscope (AFM) (Multimode IIIa, Digital Instruments) was operated in tapping mode to acquire images of the surfaces of polymer:PC$_{70}$BM blend layers.

2.3.1. 6-(2-Ethylhexyloxy)-1-iodonaphthalene (*3*)

5-Iodo-2-naphthol (4.45 g, 16.48 mmol), anhydrous potassium carbonate (6.910 g, 50 mmol), and 2-ethylhexyl bromide (9.657 g, 50 mmol) were dissolved in anhydrous *N*,*N*-dimethylformamide (DMF, 50 mL). The solution was heated at 70 °C and stirred for 16 h under nitrogen atmosphere. The reaction mixture was then poured into water and extracted with ethyl acetate. The organic layer was then successively washed with water and dried over anhydrous $MgSO_4$. The solvent was evaporated and the residue was purified by column chromatography on silica gel with 1:4 ethyl acetate/hexane as an eluant to yield orange viscous liquid (5.859 g, 93%).

^{1}H NMR ($CDCl_3$, 400 MHz, ppm): 7.95 (d, 1H, *J* = 9.2 Hz), 7.89 (dd, 1H, *J* = 7.4, 1.2 Hz), 7.68 (d, 1H, *J* = 8 Hz), 7.20 (1H, dd, *J* = 9.2, 2.4 Hz), 7.08 (1H, t, *J* = 8 Hz), 7.05 (1H, d, *J* = 2.4 Hz), 3.95 (2H, dd, *J* = 5.8, 1.2 Hz), 1.78 (1H, m), 1.59–1.40 (4H, m), 1.35–1.30 (4H, m), 1.00–0.85 (6H, m). ^{13}C NMR ($CDCl_3$, 100 MHz, ppm): 157.92, 135.20, 134.90, 133.57, 129.72, 127.72, 127.20, 120.65, 106.88, 99.16, 70.71, 39.34, 30.56, 29.09, 23.91, 23.04, 14.08, 11.12. Anal. Calcd. for $C_{18}H_{23}IO$: C, 56.55; H, 6.06; I, 33.20; O, 4.19. Found: C, 57.76; H, 6.06. ESI-MS: N/A [56].

2.3.2. Di(1-(6-(2-ethylhexyloxy)naphthyl))phenylamine (*4*)

The synthesis of the compound **4** was carried out following a modified literature procedure [57]. To a two-neck round-bottomed flask (RBF) equipped with a reflux condenser, **3** (6.6 g, 17.26 mmol), aniline (0.723 g, 7.76 mmol), tris(dibenzylideneacetone)dipalladium ($Pd_2(dba)_3$) (0.158 g, 0.17 mmol), *tri-tert*-butylphosphine (P(*t*Bu)$_3$) (0.69 mL, 1 M in toluene), sodium *tert*-butoxide (NaO*t*Bu) (2.322 g, 24.16 mmol), and anhydrous toluene (100 mL) were added and stirred at 90 °C for 24 h under nitrogen atmosphere. The mixture was poured into water and extracted with ethyl acetate. After drying over anhydrous $MgSO_4$, the solvent was evaporated. The residue was purified by column chromatography on silica gel with 1:4 dichloromethane/hexane as an eluant to yield greenish yellow viscous liquid (4.017 g, 86%).

^{1}H NMR (DMSO-*d*$_6$, 400 MHz, ppm): 7.79 (2H, d, *J* = 9.6 Hz), 7.65 (2H, d, *J* = 8.4 Hz), 7.37 (2H, d, *J* = 2.4 Hz), 7.35 (2H, d, *J* = 7.6 Hz), 7.11 (2H, t, *J* = 8.2 Hz), 7.02 (2H, dd, *J* = 9.4, 2.4 Hz), 6.95 (2H, dd, *J* = 7.4, 1.2 Hz), 6.83 (1H, t, *J* = 7.2 Hz), 6.54 (2H, dd, *J* = 8.6, 1.2 Hz), 3.94 (4H, d, *J* = 6 Hz), 1.79–1.62 (2H, m), 1.55–0.121 (16H, m), 0.91–0.84 (12H, m). ^{13}C NMR (DMSO-*d*$_6$, 100 MHz, ppm): 156.84, 149.96, 144.12, 136.36, 129.07, 126.80, 125.12, 124.66, 124.60, 122.13, 120.52, 119.62, 118.96, 107.50, 69.96, 38.60, 29.92, 28.39, 23.31, 22.49, 13.92, 10.86. Anal. Calcd. for $C_{42}H_{51}NO_2$: C, 83.82; H, 8.54; N, 2.33; O, 5.32. Found: C, 83.78; H, 8.64; N, 2.31. ESI-MS: 624.38 for [M + Na]$^+$ (Calcd for [M]: 601.39).

2.3.3. Di(1-(4-bromo-6(2-ethylhexyloxy)naphthyl))phenylamine (*5*)

To a solution of compound 4 (5.576 g, 9.26 mmol) in anhydrous DMF (60 mL), *N*-bromosuccinimide (NBS) (3.38 g, 18.99 mmol) was added. The mixture was stirred for 24 h, then poured into water and extracted with ethyl acetate. The extract was successively washed with water and dried over anhydrous $MgSO_4$. The solvent was evaporated and the residue was purified by column chromatography on silica gel with 1:4 dichloromethane/hexane as an eluant to afford the product as a yellowish viscous liquid (5.276 g, 75%).

^{1}H NMR ($CDCl_3$, 400 MHz, ppm): 7.89 (2H, d, *J* = 9.2 Hz), 7.58 (2H, d, *J* = 8 Hz), 7.49 (2H, d, *J* = 2.8 Hz), 7.10 (2H, t, *J* = 7.8 Hz), 6.99 (2H, dd, *J* = 9.2, 2.4 Hz), 6.70 (2H, dd, *J* = 8.6, 1.2 Hz), 3.98 (4H, d, *J* = 5.6 Hz), 1.85–1.70 (2H, m), 1.59–1.38 (8H, m), 1.37–1.26 (8H, m), 1.02–0.81 (12H, m). ^{13}C NMR ($CDCl_3$, 100 MHz, ppm): 158.64, 150.04, 144.64, 134.78, 130.53, 129.05, 126.33, 126.20, 122.70, 121.36, 120.90, 120.03, 118.11, 106.78, 70.48, 39.28, 30.60, 29.12, 23.94, 23.03, 14.08, 11.18. Anal. Calcd. for $C_{42}H_{49}Br_2NO_2$: C, 66.41; H, 6.50; Br, 21.04; N, 1.84; O, 4.21. Found: C, 66.64; H, 6.46; N, 1.98. ESI-MS: 780.20 for [M + Na]$^+$ (Calcd for [M]: 757.21).

2.3.4. Di(1-(4-(4,4,5,5-tetramethyl-1,3,2-dioxaborolan-2-yl)-6(2-ethylhexyloxy)naphthyl))-phenylamine (*1*)

To a solution of compound **7** (6.675 g, 8.79 mmol) in 20 mL of anhydrous THF at −78 °C, 8.09 mL (20.22 mmol) of *n*-butyllithium (2.5 M in hexane) was added by syringe. The mixture was stirred at −78 °C for 2 h, and then 2-isopropoxy-4,4,5,5-tetramethyl-1,3,2-dioxaborolane (4.13 mL, 20.22 mmol) was added to the solution. After 1 h, the reaction mixture was warmed to room temperature and stirred for further 12 h. The reaction mixture was poured into water, extracted with diethyl ether, and dried over anhydrous $MgSO_4$. The solvent was evaporated and the residue was purified by column chromatography on silica gel with 1:5 hexane/toluene as an eluant to afford the product as a yellowish viscous liquid (5.404 g, 72%).

^{1}H NMR ($CDCl_3$, 400 MHz, ppm): 8.39 (2H, d, *J* = 2.4 Hz), 8.04 (2H, d, *J* = 9.2 Hz), 8.02 (2H, d, *J* = 8.4 Hz), 7.19 (2H, t, *J* = 8 Hz), 7.09 (2H, d, *J* = 7.6 Hz), 7.05 (2H, dd, *J* = 9.4, 2.4 Hz), 6.96 (1H, t, *J* = 7.2 Hz), 6.87 (2H, d, *J* = 7.6 Hz), 4.11 (4H, d, *J* = 6 Hz), 1.97–1.91 (2H, m), 1.70–1.42 (40H, m), 1.08–0.97 (12H, m). ^{13}C NMR ($CDCl_3$, 100 MHz, ppm): 157.61, 150.25, 148.21, 140.52, 136.55, 128.91, 128.79, 128.12, 125.88, 124.67, 121.67, 121.37, 118.55, 108.05, 83.39, 70.34, 38.96, 30.50, 28.91, 24.94, 23.83, 23.06, 14.07, 10.98. Anal. Calcd. for $C_{54}H_{73}B_2NO_6$: C, 75.97; H, 8.62; B, 2.53; N, 1.64; O, 11.24. Found: C, 76.23; H, 8.77; N, 1.74. ESI-MS: 876.55 for [M + Na]$^+$ (Calcd for [M]: 853.56).

2.3.5. Poly[4,4-(di(1-(6-(2-ethylhexyl)naphthyl))phenylamine)-alt-5,5-(4′,7′-di-2-thienyl-2′,1′,3′-benzothiadiazole)] (***PDNPADTBT***)

In a two-necked RBF equipped with a condenser, monomer **1** (0.338 g, 0.395 mmol), monomer **6** (0.181 g, 0.395 mmol), palladium(II) acetate ($Pd(OAc)_2$) (5.3 mg, 0.008 mmol), and tricyclohexyl phosphine (3.3 mg, 0.012 mmol) were dissolved in toluene (3.1 mL). To this solution, tetramethyl ammonium hydroxide (Me_4NOH) (0.256 g, 1.74 mmol, 20 wt% in water) was added, and then the reaction mixture was vigorously stirred at 90 °C for 24 h under nitrogen. 2-Bromothiophene and phenylboronic acid were added at the end of the reaction to endcap the polymer chain end. After cooling to room temperature, the reaction mixture was poured into methanol, and filtered. The precipitate was washed in Soxhlet apparatus with methanol, acetone, and chloroform for 24 h, respectively. The chloroform fraction was condensed, and precipitated in methanol. The final product was obtained after drying in vacuo at 60 °C, yielding 0.231 g (65%).

IR (KBr, cm^{-1}): 2957, 2925, 2860, 1619, 1579, 1490, 1437, 1361, 1322, 1266, 1221, 1028, 876, 746, 695. ^1H NMR ($CDCl_3$, 400 MHz, ppm): 8.24 (2H, br), 8.05 (2H, d, $J = 9.2$ Hz), 7.93 (2H, br), 7.74 (2H, s), 7.50 (2H, br), 7.38 (2H, br), 7.20–7.07 (4H, m), 7.05 (2H, d, $J = 8.8$ Hz), 6.93–6.77 (3H, m), 3.90 (4H, br), 1.78–1.65 (2H, m), 1.61–1.09 (16H, m), 1.01–0.64 (12H, m). ^{13}C NMR ($CDCl_3$, 100 MHz, ppm): 158.06, 157.22, 152.66, 150.29, 145.31, 143.99, 139.23, 134.72, 129.19, 129.05, 128.25, 128.18, 128.06, 126.38, 125.77, 125.47, 121.93, 121.13, 120.71, 119.04, 105.78, 70.34, 39.31, 30.58, 29.12, 23.89, 23.01, 14.06, 11.19. Anal. Calcd. for $C_{56}H_{57}N_3O_2S_3$: C, 74.71; H, 6.38; N, 4.67; O, 3.55; S, 10.69. Found: C, 74.08; H, 6.52; N, 4.28; O, 3.49; S, 10.06.

2.3.6. *Poly[4,4-(di(1-(6-(2-ethylhexyl)naphthyl))phenylamine)-alt-5,5-(4′,7′-di-2-thienyl-2′,1′,3′-benzoselenadiazole)]* (***PDNPADTBS***)

In a two-necked RBF equipped with a condenser, monomer **1** (0.3 g, 0.352 mmol), monomer **6** (0.178 g, 0.352 mmol), $Pd(OAc)_2$ (4.7 mg, 0.007 mmol), and tricyclohexyl phosphine (3.0 mg, 0.011 mmol) were dissolved in toluene (2.7 mL). To this solution, Me_4NOH (0.228 g, 1.55 mmol, 20 wt% in water) was added, and then the reaction mixture was vigorously stirred at 90 °C for 24 h under nitrogen. 2-Bromothiophene and phenylboronic acid were added at the end of the reaction to endcap the polymer chain end. After cooling to room temperature, the reaction mixture was poured into methanol, and filtered. The precipitate was washed in Soxhlet apparatus with methanol, acetone, and chloroform for 24 h, respectively. The chloroform fraction was condensed, and precipitated in methanol. The final product was obtained after drying in vacuo at 60 °C, yielding 0.22 g (66%).

IR (KBr, cm^{-1}): 2955, 2924, 2861, 1618, 1579, 1490, 1435, 1362, 1322, 1266, 1219, 1026, 821, 747, 693. ^1H NMR ($CDCl_3$, 400 MHz, ppm): 8.15 (2H, br), 8.05 (2H, d, $J = 9.2$ Hz), 7.86 (2H, br), 7.74 (2H, s), 7.51 (2H, br), 7.37 (2H, br), 7.18–7.09 (4H, m), 7.04 (2H, d, $J = 9.2$ Hz), 6.94–6.71 (3H, m), 3.90 (4H, br), 1.78–1.65 (2H, m), 1.60–1.09 (16H, m), 1.01–0.64 (12H, m). ^{13}C NMR ($CDCl_3$, 100 MHz, ppm): 158.22, 158.01, 157.19, 150.29, 145.23, 144.26, 139.55, 134.71, 129.15, 129.02, 128.35, 127.94, 127.74, 127.23, 126.34, 125.65, 125.48, 121.92, 121.11, 120.68, 118.98, 105.84, 70.32, 39.31, 30.57, 29.11, 23.88, 23.04, 14.05, 11.19. Anal. Calcd. for $C_{56}H_{57}N_3O_2S_2Se$: C, 71.01; H, 6.07; N, 4.44; O, 3.38; S, 6.77; Se, 8.34. Found: C, 71.21; H, 6.17; N, 4.16; O, 3.38; S, 6.28.

3. Results and discussion

3.1. *Synthesis and characterization*

The synthesis of triarylamine-containing monomer **1** was carried out as shown in Scheme 1. Compound **2** was prepared by azotation and halogenations of 5-amino-2-naphthol [53]. Before palladium-catalyzed arylation reaction, the hydroxyl group of compound **2** was reacted with 2-ethylhexyl bromide to endow solubility of the polymer to form compound **3**. Then the compound **3** was reacted with 0.45 equivalents of aniline to result in the triarylamine compound **4** [57]. The dibromo compound **5** was synthesized by bromination of compound **4** with *N*-bromosuccinimide (NBS), then lithiation of compound **5** with *n*-butyllithium (*n*-BuLi) and quenching with 2-isopropoxy-4,4,5,5-tetramethyl-1,3,2-dioxaborolane produced a desired monomer **1**. The electron-deficient dibromo monomers consisting of BT and BS units were also synthesized following the literature procedures [49,54,55].

The alternating copolymers were synthesized via palladium-catalyzed Suzuki coupling reaction of the electron-rich monomer **1** and the electron-deficient monomers **6** and **7**. The synthetic route and structures of alternating copolymer are shown in Scheme 2. The obtained copolymers were purified by reprecipitation in methanol and Soxhlet extraction with methanol and acetone to remove catalyst and low molecular weight polymers. The copolymers showed good solubility in common organic solvents, such as chloroform, toluene, and chlorobenzene at room temperature. The chemical structure of the copolymers was confirmed by ^1H, ^{13}C nuclear magnetic resonance (NMR) spectroscopy (Fig. S1, S2), FTIR (Fig. S3), and elemental analysis. All the data is provided in Supporting Information. The number-average molecular weights (M_n) of **PDNPADTBT** and **PDNPADTBS** were determined by size exclusion chromatography (SEC) using linear polystyrene standards and

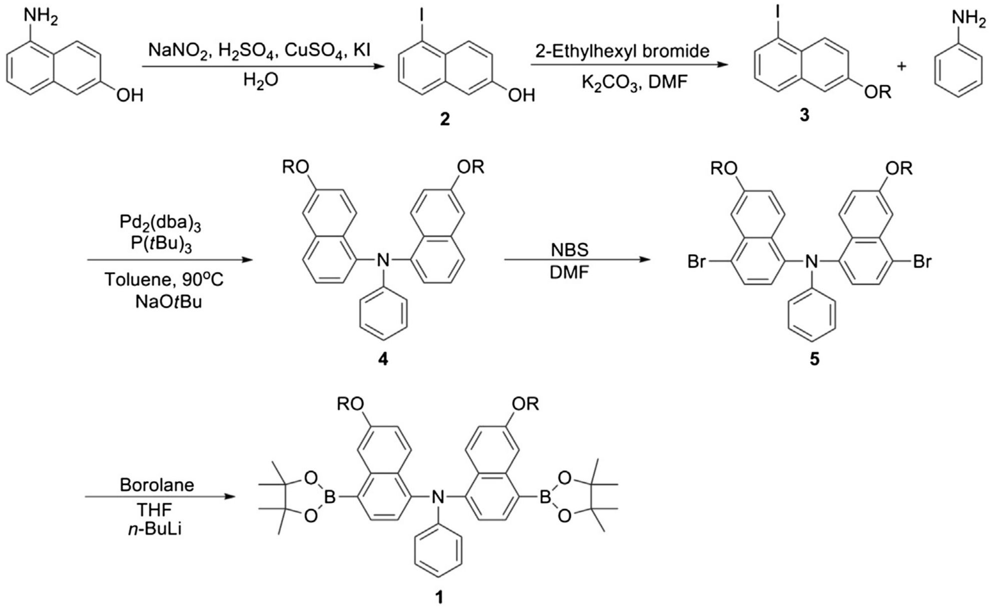

Scheme 1. Synthetic routes of monomer **1**.

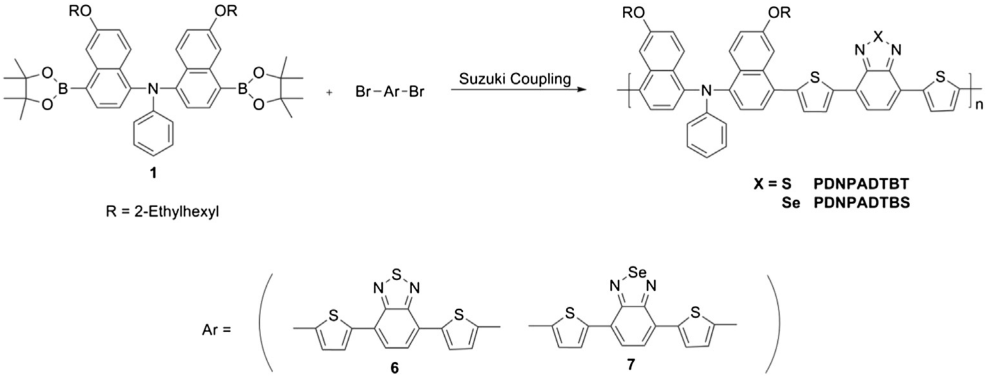

Scheme 2. Synthetic route of copolymers.

were estimated to be 10,900 ($M_w/M_n = 1.85$), 10,300 ($M_w/M_n = 1.89$), respectively (Fig. S4).

Thermal properties of the copolymers were investigated by differential scanning calorimetry (DSC) and thermogravimetric analysis (TGA) under nitrogen atmosphere. As shown in Fig. 2 and Table 1, these copolymers lost less than 5% of their weight up to 406 (**PDNPADTBT**) and 369 °C (**PDNPADTBS**), the glass transition temperatures (T_g) of the copolymers appeared at 151 (**PDNPADTBT**) and 137 °C (**PDNPADTBS**). No crystallization or melting transition was observed upon further heating beyond the T_g. The molecular weights and thermal properties are summarized in Table 1.

3.2. Optical properties

Normalized UV-vis absorption spectra of the copolymers in chloroform solutions and films are shown in Fig. 3, and optical properties of the copolymers are summarized in Table 2. The copolymers exhibited short-wavelength absorption at ~400 nm corresponding to the π–π* transition of their conjugated backbone and long-wavelength absorption which is attributed to intramolecular charge transfer (ICT) between the electron-rich monomer **1** and the electron-deficient BT derivatives. The maximum absorption spectra of **PDNPADTBT** and **PDNPADTBS** in solution appeared at 504 and 540 nm, while those in films at 521 and 558 nm, respectively. The absorption spectra in the solid state of copolymers were more red-shifted than that of the corresponding spectra in solution indicating strong interchain interaction in the solid state. Although the kinked structure of the triarylamine moiety tends to reduce the interchain interaction, we posit that incorporation of two thiophene rings at both ends of BT and BS units generated a more planar backbone structure and facilitated association between chains. The maximum absorption spectra of **PDNPADTBS** exhibited greater bathochromic shift compared with the **PDNPADTBT**, due to the larger size and more electron-rich character of the selenium atom than that of sulfur [50,58,59]. However, PDNPADTBT showed better absorption coefficient than PDNPADTBS at the long-wavelength region as shown in Fig. S5 and it was well matched with previous report [50]. The optical band gaps of the copolymer, which were calculated from the onset absorption of the film, were 1.93 (**PDNPADTBT**) and 1.81 eV (**PDNPADTBS**).

3.3. Electrochemical properties

The electrochemical properties of the copolymers also were investigated by cyclic voltammetry (CV) with Bu_4NBF_4 (0.1 M in

Table 1
Molecular weights and thermal properties of the copolymers.

Copolymer	Yield (%)	M_n[a] (10^{-3})	M_w[a] (10^{-3})	PDI	T_d[b] °C	T_g[c] °C
PDNPADTBT	65	10.9	20.2	1.85	406	151
PDNPADTBS	66	10.3	19.5	1.89	369	137

[a] Molecular weights and polydispersity index (PDI) values were measured by SEC using THF as an eluant, polystyrene as a standard.

[b] T_d exhibited 5% weight loss temperature of the polymers measured by TGA at a heating rate of 10 °C/min under nitrogen.

[c] Glass transition temperature determined by a second heating DSC curve under nitrogen, at a heating rate of 10 °C/min.

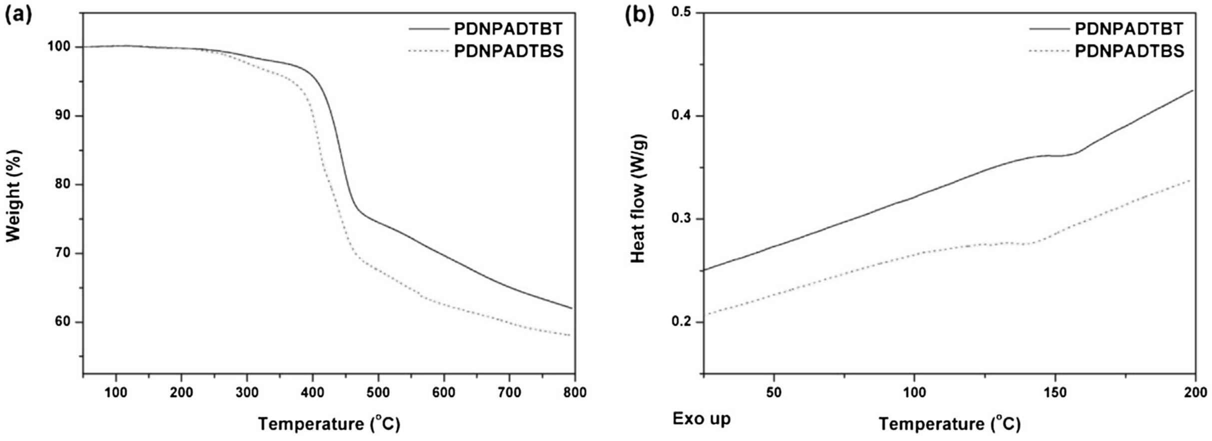

Fig. 2. TGA plot (a) and DSC plot (b) of the copolymers.

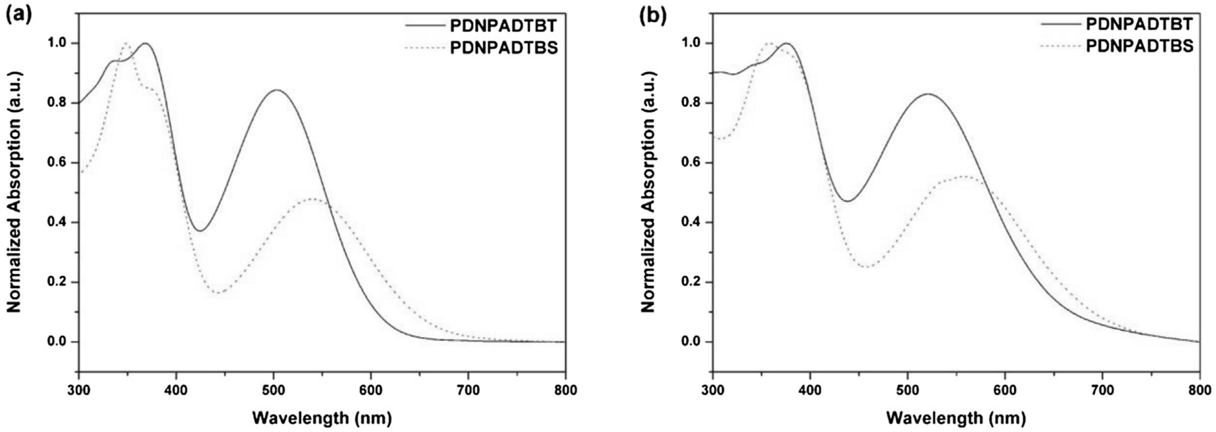

Fig. 3. Normalized UV-vis absorption spectra of the copolymers (a) in chloroform and (b) in film.

acetonitrile) at a scan rate of 50 mV s^{-1} under nitrogen. The Pt electrode coated with the polymer film was used as a working electrode and the Ag/AgNO$_3$ electrode was used as a reference electrode. The cyclic voltammograms of the copolymers are shown in Fig. 4 and the results are summarized in Table 2. The HOMO levels of the copolymers are calculated from the onset oxidation potentials according to the equation, $E_{\mathrm{HOMO}} = [-(E_{\mathrm{onset}} - E_{\mathrm{onset}}(\mathrm{Fc/Fc^+}\ \mathrm{vs.}\ \mathrm{Ag/Ag^+})) - 4.8]$ eV, relative to the ferrocene/ferrocenium (Fc/Fc$^+$) redox system, whose potential is assumed to be −4.8 eV relative to vacuum [60]. The LUMO energy levels of the copolymers were calculated from the HOMO energy levels and the optical band gap using the equation, $E_{\mathrm{LUMO}} = E_{\mathrm{HOMO}} + E_g^{\mathrm{opt}}$. The calculated HOMO energy values of **PDNPADTBT** and **PDNPADTBS** were −5.48 and −5.45 eV, and the LUMO energy values were −3.55 and −3.64 eV, respectively. The HOMO levels of copolymers were not raised apparently despite of the presence of different acceptors. However, **PDNPADTBS** showed lower LUMO energy levels than those of **PDNPADTBT**, and this result indicated that BS was more effective on lowering the LUMO level of copolymer as previously reported [50,61,62]. Intriguingly, the copolymers exhibited low HOMO levels, which allow PSCs to have high V_{oc} [63]. Compared with previous polymer systems composed of electron-rich triphenylamine and electron-deficient BT derivatives, such low HOMO levels of copolymers may be originated from the naphthalene unit introduced into the triarylamine [36,41,44,45].

3.4. Photovoltaic properties

The photovoltaic properties of triarylamine-based alternating copolymers were investigated using the bulk heterojunction photovoltaic devices which had a layered structure of ITO/PEDOT-PSS (40 nm)/polymers-PC$_{70}$BM (100 nm)/LiF (1 nm)/Al (100 nm) (ITO = indium tin oxide, PEDOT = poly(3,4-ethylenedioxythiophene), PSS = poly(styrene sulfonate)). The copolymer-PC$_{70}$BM blend in *o*-dichlorobenzene (40 mg/ml) was spin-coated as an active layer onto the PEDOT-PSS layer. All devices were tested without thermal annealing. In the polymer-fullerene blend system with intercalation, high level of fullerene loading is needed to create the optimum phase separation [64]. Therefore, initial photovoltaic systems were fabricated with the copolymer-PC$_{70}$BM blended solutions prepared in a weight ratio of 1:4 (w/w). AFM image of the copolymer-PC$_{70}$BM blend films was shown in SI (Fig. S6) and the surfaces of both blend films were similarly homogeneous. The J–V characteristics of the devices under the illumination of AM 1.5G (100 mW/cm^2) are shown in Fig. 5 and summarized in Table 3. The highest PCE of 2.0% was obtained from the **PDNPADTBT**-PC$_{70}$BM solar cell with a V_{oc} of 0.92 V, a J_{sc} of 6.8 mA/cm^2, and a fill factor (FF) of 31.7%. Under the same condition, a slightly lower PCE of 1.5% was observed from the **PDNPADTBS**-PC$_{70}$BM solar cell with a V_{oc} of 0.88 V, a J_{sc} of 5.6 mA/cm^2, and a FF of 31.2%. The slightly lower V_{oc} of PDNPADTBS-PC$_{70}$BM is probably because of the higher HOMO energy level of PDNPADTBS. It is noteworthy that the V_{oc} of **PDNPADTBT** and **PDNPADTBS** exhibited a value close to 0.9 V, which is comparable to the best result of poly(2,7-carbazole) derivatives reported in the literature,

Table 2
Electrochemical and optical properties of the copolymers.

Copolymer	λ_{max}[a] (nm)	λ_{max}[a] (nm)	E_g^{opt}[b]	$E_{\mathrm{ox/onset}}$	E_{HOMO}[c]	E_{LUMO}[d]
	Solution	Film	(eV)	(V)	(eV)	(eV)
PDNPADTBT	370, 504	376, 521	1.93	0.72	−5.48	−3.55
PDNPADTBS	350, 540	358, 558	1.81	0.69	−5.45	−3.64

[a] λ_{max}: the absorption maxima from the UV-vis spectra in chloroform solution or in film.

[b] E_g^{opt}: optical band gap determined from the absorption onset in film.

[c] E_{HOMO}: HOMO levels of the polymers was determined with the first oxidation onset potential relative to ferrocene (Fc).

[d] E_{LUMO}: LUMO energy levels of the polymers were estimated from the HOMO energy levels and E_g^{opt}.

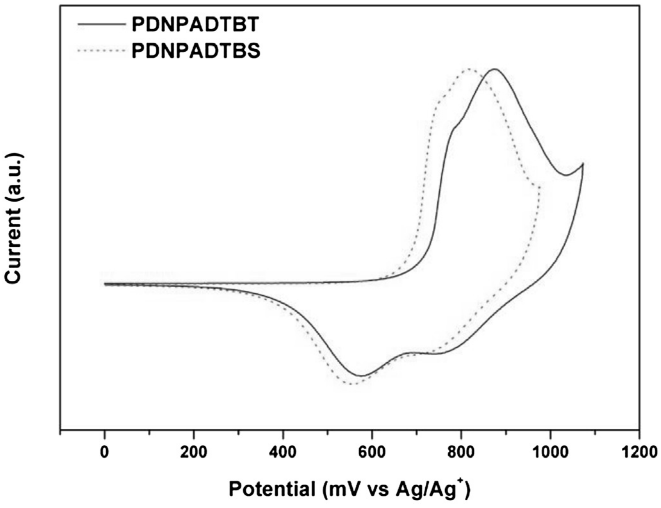

Fig. 4. Cyclic voltammograms of the copolymers.

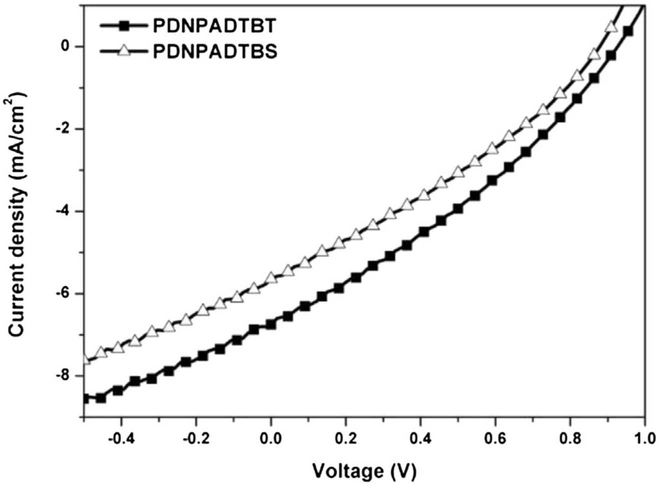

Fig. 5. *J-V* characteristics of PSCs with an active layer of copolymer-$PC_{70}BM$ (1:4, w/w) mixture under AM 1.5G illumination (100 mW/cm^2).

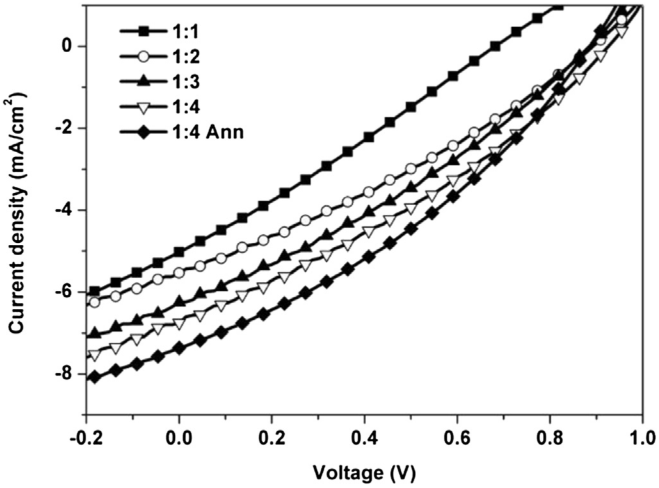

Fig. 7. Characteristics of PSCs at various **PDNPADTBT**/$PC_{70}BM$ weight ratios (AM 1.5G illumination at 100 mW/cm^2).

Table 3
Photovoltaic properties of triarylamine-based PSCs processed with copolymer-$PC_{70}BM$ (1:4, w/w) blend in dichlorobenzene.

Copolymer-$PC_{70}BM$ (1:4)	V_{oc} (V)	J_{sc} (mA/cm^2)	FF (%)	PCE[a] (%)
PDNPADTBT	0.92	6.8	31.7	2.0
PDNPADTBS	0.88	5.6	31.2	1.5

[a] Maximum values.

indicating that the low HOMO energy level is one of the important factor to obtain the high V_{oc} values of PSCs [10,47,63,65]. Fig. 6(a) shows the UV-vis absorption spectra of copolymer-$PC_{70}BM$ blend films at 1:4 weight ratio. Although PDNPADTBS-$PC_{70}BM$ blend film had a bathochromic absorption shift compared to PDNPADTBT-$PC_{70}BM$ blend film as expected from the absorption spectra of the copolymers, much larger absorption coefficients of PDNPADTBT than PDNPADTBS in the range of 450–600 nm (Fig. S5) appeared to dominate efficiency of the PSC up to 600 nm with negligible difference from 600 to 700 nm. Thus higher performance of the PSC consisting of PDNPADTBT was attributed to lower HOMO energy level and higher absorption coefficient of PDNPADTBT than PDNPADTBS.

By selecting the **PDNPADTBT**-$PC_{70}BM$ solar cell which showed a better performance, effects of donor-acceptor blend ratios and thermal annealing on the photovoltaic response of the PSCs were further investigated. The photovoltaic properties of the polymer blends **PDNPADTBT**-$PC_{70}BM$ in various weight compositions (1:1, 1:2, 1:3, and 1:4 w/w) were estimated under same conditions and current–voltage characteristic of these devices are shown in Fig. 7 and summarized in Table 4. Power conversion efficiency (PCE) values of the devices ranged from 0.94% (1:1 w/w) to 2.0% (1:4 w/w) according to variation in the composition. The lower ratios of $PC_{70}BM$ in the polymer blends led to reduction in J_{sc} values because of the inefficient charge separation and electron transporting properties, and considerable reduction of V_{oc} and FF values was observed when the weight composition became 1:1. The effect of thermal annealing on blends **PDNPADTBT**-$PC_{70}BM$ (1:4 w/w) solar cell was also investigated. It was found that the best PCE of 2.2% was obtained when the device was annealed under 140 °C for 20 min. The morphologies of the **PDNPADTBT**-$PC_{70}BM$ blend films before and after heat treatment were estimated by atomic force microscopy (AFM) as shown in Fig. 8. Both films possessed smooth surfaces, with a low root mean square (RMS) roughness of 0.367 and 0.333 nm, respectively. However, smoother surface was obtained after annealing and showed more uniform morphology without significant phase separation. Since interpenetrating polymer-PCBM networks with a smaller domain size is known to be better for efficient charge transfer and separation, we ascribe that formation

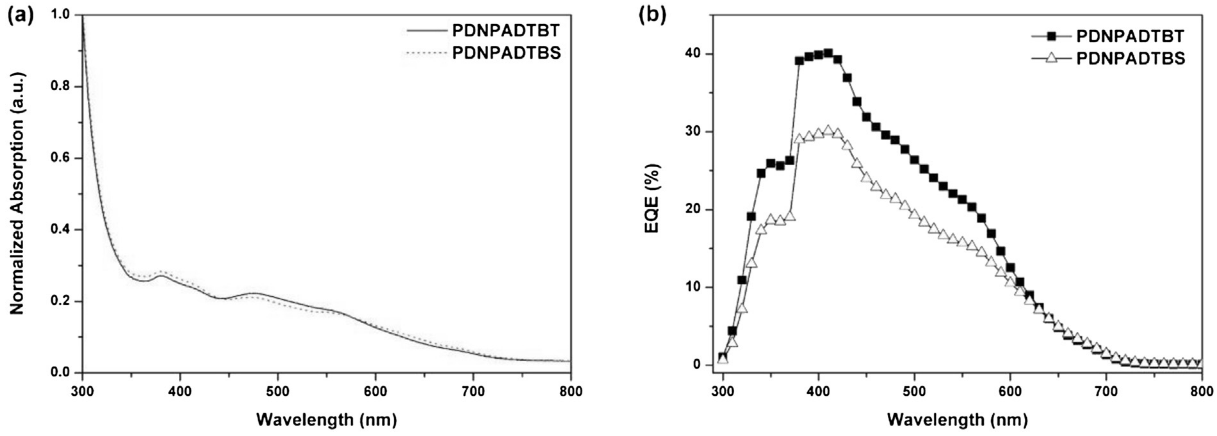

Fig. 6. (a) Absorption spectra of copolymer-$PC_{70}BM$ (1:4, w/w) blend films spin-coated from dichlorobenzene and (b) EQE curves of copolymer-$PC_{70}BM$ based PSCs.

Table 4
Photovoltaic properties of PSCs at various **PDNPADTBT**/PC$_{70}$BM weight ratios (AM 1.5G illumination at 100 mW/cm^2).

Annealing temp. (°C)	Solar cell performance				
	Ratio	V_{oc} (V)	J_{sc} (mA/cm^2)	FF (%)	PCE[a] (%)
As-casted	1:1	0.68	5.0	27.4	0.94
As-casted	1:2	0.89	5.5	30.5	1.5
As-casted	1:3	0.88	6.2	31.6	1.7
As-casted	1:4	0.92	6.8	31.7	2.0
Annealed (140 °C)	1:4	0.88	7.4	34.4	2.2

[a] Maximum values.

of the more uniform phase separated blend by thermal annealing leads to improvement of J_{sc}, FF, and PCE [66,67]. PDNPADTBT-PC$_{70}$BM solar cell showed improved V_{oc} and J_{sc} values compared to previously reported copolymers composed of triphenylamine and DTBT derivatives supporting our approach to obtain high performance PSCs [36,40,41].

4. Conclusion

In summary, **PDNPADTBT** and **PDNPADTBS** were successfully synthesized as new triarylamine-based alternating copolymers and these copolymers exhibited excellent solubility in common organic solvents. The electronic structures of the copolymers were effectively controlled via ICT between the electron-rich triarylamine and the electron-deficient BT or BS derivatives. **PDNPADTBT** and **PDNPADTBS** exhibited its maximum absorption at 521 and 558 nm and the optical band gaps of 1.93 and 1.81 eV, respectively. The HOMO energy levels of **PDNPADTBT** and **PDNPADTBS** were −5.48 and −5.45 eV indicating that the HOMO energy levels were effectively lowered by introduction of naphthalene into triarylamine which would be beneficial for air stability and high V_{oc}. The photovoltaic properties of the copolymers were estimated with copolymer-PC$_{70}$BM blended system. Both the blend systems showed remarkably high V_{oc} close to 0.9 V, and it was found that the highest PCE of 2.2% with V_{oc} = 0.88 V and J_{sc} = 7.4 mA/cm^2 under AM 1.5G was obtained after the heat treatment from **PDNPADTBT**. Although they had high V_{oc}, the PCE of PSCs was not sufficiently high due to limited solar absorption and a low FF. Currently we are exploring other electron-deficient acceptor which could reduce the band gap of the copolymers to further improve solar cell performances.

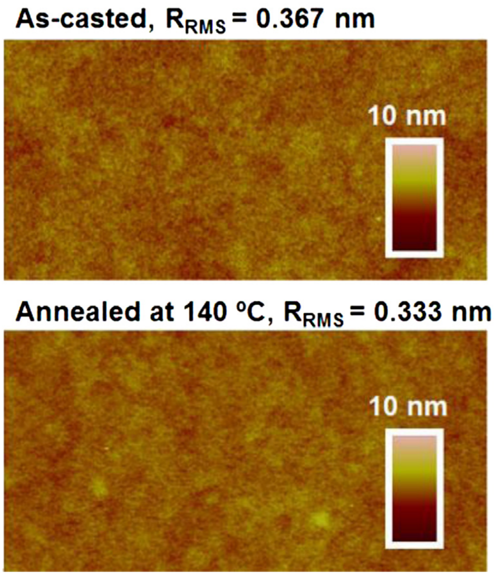

Fig. 8. AFM topographic images (5 × 2.5 μm^2) of the blended film (**PDNPADTBT**/PC$_{70}$BM 1:4, w/w) before and after heat treatment at 140 °C for 20 min.

Acknowledgments

This work was supported by a NRF grant funded by MSIP through the NRL (R0A-2008-000-20121-0) and the ERC (R11-2007-050-00000-0) programs.

Appendix A. Supplementary data

Supplementary data related to this article can be found at http://dx.doi.org/10.1016/j.polymer.2014.08.018.

References

[1] Li C, Liu M, Pschirer NG, Baumgarten M, Müllen K. Chem Rev 2010;110:6817–55.
[2] Morton O. Nature 2006;443:19–22.
[3] Mayer AC, Scully SR, Hardin BE, Rowell MW, McGehee MD. Mater Today 2007;10:28–33.
[4] Dhere NG. Sol Energy Mater Sol Cells 2007;91:1376–82.
[5] Service RF. Science 2008;319:718–20.
[6] Fthenakis VM. Renew Sust Energ Rev 2004;8:303–34.
[7] Yu G, Gao J, Hummelen JC, Wudl F, Heeger AJ. Science 1995;270:1789–91.
[8] Brabec CJ, Sariciftci NS, Hummelen JC. Adv Funct Mater 2001;11:15–26.
[9] Sariciftci NS, Smilowitz L, Heeger AJ, Wudl F. Science 1992;258:1474–6.
[10] Park SH, Roy A, Beaupre S, Cho S, Coates N, Moon JS, et al. Nat Phot 2009;3:297–302.
[11] Wang E, Ma Z, Zhang Z, Vandewal K, Henriksson P, Inganäs O, et al. J Am Chem Soc 2011;133:14244–7.
[12] Price SC, Stuart AC, Yang L, Zhou H, You W. J Am Chem Soc 2011;133:4625–31.
[13] Zhou H, Yang L, Price SC, Knight KJ, You W. Angew Chem Int Ed 2010;49:7992–5.
[14] Chen H-Y, Hou J, Zhang S, Liang Y, Yang G, Yang Y, et al. Nat Phot 2009;3:649–53.
[15] Huo L, Zhang S, Guo X, Xu F, Li Y, Hou J. Angew Chem Int Ed 2011;50:9697–702.
[16] Thelakkat M. Macromol Mater Eng 2002;287:442–61.
[17] Shirota Y. J Mater Chem 2005;15:75–93.
[18] Shirota Y, Kageyama H. Chem Rev 2007;107:953–1010.
[19] Iwan A, Sek D. Prog Polym Sci 2011;36:1277–325.
[20] Ning Z, Tian H. Chem Commun 2009:5483–95.
[21] Roncali J. Acc Chem Res 2009;42:1719–30.
[22] He C, He Q, Yi Y, Wu G, Bai F, Shuai Z, et al. J Mater Chem 2008;18:4085–90.
[23] Zhang J, Yang Y, He C, He Y, Zhao G, Li Y. Macromolecules 2009;42:7619–22.
[24] Wu G, Zhao G, He C, Zhang J, He Q, Chen X, et al. Sol Energy Mater Sol Cells 2009;93:108–13.
[25] Shang H, Fan H, Shi Q, Li S, Li Y, Zhan X. Sol Energy Mater Sol Cells 2010;94:457–64.
[26] Liu Q, Jiang K, Guan B, Tang Z, Pei J, Song Y. Chem Commun 2011;47:740–2.
[27] Deng D, Yang Y, Zhang J, He C, Zhang M, Zhang Z-G, et al. Org Electron 2011;12:614–22.
[28] Zhang Z-G, Zhang K-L, Liu G, Zhu C-X, Neoh K-G, Kang E-T. Macromolecules 2009;42:3104–11.
[29] Huang F, Chen K-S, Yip H-L, Hau SK, Acton O, Zhang Y, et al. J Am Chem Soc 2009;131:13886–7.
[30] Mikroyannidis JA, Kabanakis AN, Balraju P, Sharma GD. Macromolecules 2010;43:5544–53.
[31] Duan C, Cai W, Huang F, Zhang J, Wang M, Yang T, et al. Macromolecules 2010;43:5262–8.
[32] Cheng Y-J, Hung L-C, Cao F-Y, Kao W-S, Chang C-Y, Hsu C-S. J Polym Sci Part A Polym Chem 2011;49:1791–801.
[33] Nie K, Tan H, Deng X, Wang Y, Chen Q, Huang Y, et al. J Polym Sci Part A Polym Chem 2013;51:4103–10.
[34] Yasuda T, Shinohara Y, Ishi-i T, Han L. Org Electron 2012;13:1802–8.
[35] Yasuda T, Suzuki T, Takahashi M, Han L. Sol Energy Mater Sol Cells 2011;95:3509–15.
[36] Yasuda T, Shinohara Y, Matsuda T, Han L, Ishi-i T. J Polym Sci Part A Polym Chem 2013;51:2536–44.
[37] Yasuda T, Shinohara Y, Matsuda T, Han L, Ishi-i T. J Mater Chem 2012;22:2539–44.
[38] Huo L, He C, Han M, Zhou E, Li Y. J Polym Sci Part A Polym Chem 2007;45:3861–71.
[39] Blankenburg L, Hager MD, Sell S, Sensfuss S, Klemm E. J Appl Polym Sci 2009;111:1850–61.

[40] Tu G, Massip S, Oberhumer PM, He X, Friend RH, Greenham NC, et al. J Mater Chem 2010;20:9231–8.

[41] Wang M, Li C, Lv A, Wang Z, Bo Z, Zhang F. Polymer 2012;53:324–32.

[42] Hindson JC, Ulgut B, Friend RH, Greenham NC, Norder B, Kotlewski A, et al. J Mater Chem 2010;20:937–44.

[43] Iwan A, Palewicz M, Chuchmala A, Gorecki L, Sikora A, Mazurek B, et al. Synt Met 2012;162:143–53.

[44] Chung DS, Park JW, Kim S-O, Heo K, Park CE, Ree M, et al. Chem Mater 2009;21:5499–507.

[45] Kim S-O, Chung DS, Cha H, Hwang MC, Park J-W, Kim Y-H, et al. Sol Energy Mater Sol Cells 2011;95:1678–85.

[46] Hou Q, Xu Y, Yang W, Yuan M, Peng J, Cao Y. J Mater Chem 2002;12:2887–92.

[47] Blouin N, Michaud A, Gendron D, Wakim S, Blair E, Neagu-Plesu R, et al. J Am Chem Soc 2007;130:732–42.

[48] Padhy H, Huang J-H, Sahu D, Patra D, Kekuda D, Chu C-W, et al. J Polym Sci Part A Polym Chem 2010;48:4823–34.

[49] Jung IH, Kim H, Park M-J, Kim B, Park J-H, Jeong E, et al. J Polym Sci Part A Polym Chem 2010;48:1423–32.

[50] Gibson GL, McCormick TM, Seferos DS. J Am Chem Soc 2011;134:539–47.

[51] Zhou E, Cong J, Hashimoto K, Tajima K. Macromolecules 2013;46:763–8.

[52] Zhao W, Cai W, Xu R, Yang W, Gong X, Wu H, et al. Polymer 2010;51:3196–202.

[53] Snyckers F, Zollinger H. Helv Chim Acta 1970;53:1294–305.

[54] Huang F, Hou L, Shen H, Jiang J, Wang F, Zhen H, et al. J Mater Chem 2005;15:2499–507.

[55] Li X, Zeng W, Zhang Y, Hou Q, Yang W, Cao Y. Eur Polym J 2005;41:2923–33.

[56] We were not able to obtain a mass spectrum of the corresponding compound via ESI-MS.

[57] Nomura M, Shibasaki Y, Ueda M, Tugita K, Ichikawa M, Taniguchi Y. Macromolecules 2004;37:1204–10.

[58] Yang R, Tian R, Hou Q, Yang W, Cao Y. Macromolecules 2003;36:7453–60.

[59] Huang F, Hou L, Shen H, Yang R, Hou Q, Cao Y. J Polym Sci Part A Polym Chem 2006;44:2521–32.

[60] de Leeuw DM, Simenon MMJ, Brown AR, Einerhand REF. Synth Met 1997;87:53–9.

[61] Yasuda T, Imase T, Yamamoto T. Macromolecules 2005;38:7378–85.

[62] Özkut M, İpek H, Karabay B, Cinhaner A, Önal AM. Polym Chem 2013;4:2457–63.

[63] Scharber MC, Mühlbacher D, Koppe M, Denk P, Waldauf C, Heeger AJ, et al. Adv Mater 2006;18:789–94.

[64] Mayer AC, Toney MF, Scully SR, Rivnay J, Brabec CJ, Scharber M, et al. Adv Funct Mater 2009;19:1173–9.

[65] Khlyabich PP, Burkhart B, Thompson BC. J Am Chem Soc 2011;133:14534–7.

[66] Beaujuge PM, Fréchet JMJ. J Am Chem Soc 2011;133:20009–29.

[67] Vacar D, Maniloff ES, McBranch DW, Heeger AJ. Phys Rev B 1997;56:4573–7.